Multi-physics simulations using single-physics software and generic coupling

Antoine Alexandre Journeaux

Laboratoire de Génie Électrique de Paris
11 rue Joliot Curie, 91192 Gif-sur-Yvette, France
antoine.journeaux@lgep.supelec.fr

ABSTRACT. *Generic projection methods allow, starting from existing computer programs, the modeling of various type of problems. The present study is an application of the mesh-to-mesh data transfer method which aims at solving a coupled magneto-thermal problem using two, seemingly unrelated, computer codes. After a brief description of the projection methods, a numerical comparison in terms of local and global errors is proposed. Then an analytical test case is used to perform benchmarks on coupled problem modeling, hence highlighting the influence of the data processing on the quality of the solution.*

RÉSUMÉ. *Les méthodes génériques de projections permettent, à l'aide de codes de calculs existants, de modéliser différents types de problèmes multi-physiques. Cette étude porte sur l'application à un problème couplé magnéto-thermique des méthodes de projections afin de faire communiquer deux codes n'étant a priori pas conçus pour cette utilisation. Après un rappel théorique sur les méthodes de projections, une comparaison numérique des erreurs introduites par chacune des méthodes est présentée. Un cas test analytique est ensuite étudié pour prouver l'applicabilité de tels couplages à des problèmes réels. Des conclusions sur les performances comparées des méthodes sont proposées.*

KEYWORDS: *coupled problems modeling, magneto-thermal problems, data projections, data interpolations, numerical methods*

MOTS-CLÉS : *modélisation des problèmes couplés, problèmes magnéto-thermiques, projections de solutions, interpolations, méthodes numériques*

DOI:10.3166/EJEE.17.95-103

1. Introduction

The unrestricted access to advanced modeling software is attractive, however these computational codes are, most of the time, physics-oriented. The need for accurate multi-physical models, along with the large increase of the computational power, revives the interest in software chainings. Coupled problems are usually modeled using "strong coupling" methods which aim at solving all the physics together. Although this "strong coupling" scheme generally presents a high convergence rate, substantial drawbacks remain (Hameyer *et al.*, 1999). First, this type of problems requires the storage of large (compared to the chaining processes) non-symmetric matrices, thus reducing the scope of usable methods. Secondly, the "strong coupling" method generally leads to nonlinear models solved using iterative methods (Ren, Razek, 1994). These major drawbacks balance the weak convergence rate of the "weak coupling" scheme relying on a successive resolution of each sub-problems. The main advantages are an easier data handling and cuts in memory consumption (Alauzet, Mehrenberger, 2009; Bernardi *et al.*, 1993; Jiao, Heath, 2004; Tsukerman, 1992).

In the present article, mesh-to-mesh data transfer methods are used to separate each physical sub-problems. This operation is performed in order to reduce the topological extension of the meshes, and to adapt the fineness to the effective variations of the solutions. The data transfer methods are first presented, then a benchmark is led to compare the efficiency of these processes. Finally, a multi-physics example illustrating the ability to compute coupled problems using multiple meshes is presented.

1.1. Interpolation

The interpolation method uses the interpolated values of u_s through the target mesh to compute the DoFs of the target function u_t. For a given class of finite elements, values of a discretized function are given by:

$$d_{t_i}^{node} = u_s(x_i), \qquad (1)$$

$$d_{t_i}^{edge} = \int_{\gamma=edge} u_s(s) \cdot d\gamma, \qquad (2)$$

$$d_{t_i}^{face} = \int_{S=face} u_s(s) \cdot n dS, \qquad (3)$$

$$d_{t_i}^{element} = \int_{V=element} u_s(s) dV, \qquad (4)$$

where d_{t_i} is the i$^{\text{th}}$ DoF of the target function and w_{t_i} its associated basis function. x_{t_i} represents the coordinates of the i$^{\text{th}}$ node of $\mathcal{T}_t$. These DoFs are given by the integral of u_s through 0, 1, 2, and 3 dimensional elements (respectively equations (1) to (4)). This interpolation method has the advantage of being fast to compute, but is not strictly conservative: the integral of the function is not preserved. Moreover, it is very diffusive and the solution is rapidly smoothed in the case of repeated transfers.

1.2. Orthogonal projection

Due to the discrete nature of the functions, u_s and u_t belong to the functional space of square-integrable functions ($\mathcal{L}^2$). A second data transfer method consists in minimizing the square of the norm of the residual ($\|u_s - u_t\|$). If $\|u_s - u_t\|^2$ is minimal one has:

$$\begin{aligned} &\partial_{d_{t_i}} \|u_t - u_s\|^2_{|\mathcal{D}_c} = 0, \ \ \forall d_{t_i},\ i = 1 \dots K_t, \\ &\|\cdot\|_{|\mathcal{D}_c} = \sqrt{\langle \cdot, \cdot \rangle_{|\mathcal{D}_c}}. \end{aligned} \tag{5}$$

Using $u_t = \sum w_{t_i}\, d_{t_i}$, the global $\mathcal{L}^2$ minimization becomes:

$$\begin{aligned} \partial_{d_{t_i}} \|u_c - u_s\|^2_{|\mathcal{D}_c} &= \partial_{d_{t_i}} \| \sum_{j=1}^{K_c} w_{t_j} d_{t_j} \ - \ u_c\|^2_{|\mathcal{D}_c}, \\ &= \partial_{d_{t_i}} \sum_{j=1}^{K_c} \|w_{t_j} d_{t_j}\|^2_{|\mathcal{D}_c} - 2\, \partial_{d_{t_i}} \sum_{j=1}^{K_c} \langle w_{t_j} d_{t_j}, u_s \rangle_{|\mathcal{D}_c} + \partial_{d_{t_i}} \|u_s\|^2_{|\mathcal{D}_c}, \\ &= 2\langle w_{t_i}, \sum_{j=1}^{K_c} w_{t_j} d_{t_j} \rangle_{|\mathcal{D}_c} - 2\langle w_{t_i}, u_s \rangle_{|\mathcal{D}_c}, \\ &= 2\langle w_{t_i}, u_c \rangle_{|\mathcal{D}_c} - 2\langle w_{t_i}, u_s \rangle_{|\mathcal{D}_c} = 0, \ \ \forall d_{t_i},\ i = 1 \dots K_t, \end{aligned} \tag{6}$$

where $\langle \cdot, \cdot \rangle$ denotes the scalar product of $\mathcal{L}^2$, and K_t represents the number of finite elements discretizing the target function. The minimization leads to the following system:

$$[M][U_t] = [N][U_s]. \tag{7}$$

$[U_s]$ and $[U_t]$ respectively represent the arrays of DoFs for the two solutions. $[M]$ and $[N]$ are two mass matrices, for which the entries are:

$$M_{i,j} = \int_{\mathcal{D}_c} w_{t_i} \cdot w_{t_j}, \tag{8a}$$

$$N_{i,j} = \int_{\mathcal{D}_c} w_{t_i} \cdot w_{s_j}. \tag{8b}$$

The resolution of this system provides the target DoFs $[U_t]$, hence u_t itself. The main difficulty of this method lies in the determination of the integral (8b) which involves basis functions of both source and target meshes.

The $\mathcal{L}^2$ minimization produces the unique function u_t which is the closest one to the source function u_s. Moreover, the properties of the Galerkin method[1] ensure

1. The Galerkin method is the underlying process used to perform the orthogonal projection.

the residual $u_t - u_s$ to be orthogonal to the space spanned by the set of the target basis functions $\{w_{t_i}\}$. Thus the integral over $\mathcal{D}_c$ of u_s and u_t are equals (global conservation property). However, the $\mathcal{L}^2$ may be locally unstable if the source function strongly varies (Jiao, Heath, 2004).

1.3. Conservative projection

This method is based on the determination, for each element $\mathcal{K}$, of the local DoFs $[Q]$ such that:

$$[M_l][Q] = \begin{bmatrix} \int\limits_{\mathcal{K}} u_s \\ \int\limits_{\mathcal{K}} D(u_s) \end{bmatrix}, \quad [M] = \begin{bmatrix} \int w_{1_x} & \cdots & \int w_{6_x} \\ \vdots & \ddots & \vdots \\ \int \text{curl}\,(w_1)_z & \cdots & \int \text{curl}\,(w_6)_z \end{bmatrix}, \quad (9)$$

where D is a differential operator. $[M_l]$ represents the integrals, within $\mathcal{K}$, of the basis functions and their differential operator (written in eq. (9) for edge elements).
This linear system determines, element by element, the local DoFs $[Q] = [d_{loc_t^1} \ \ldots \ d_{loc_t^6}]$ of the target function (u_t) such that $\int_{\mathcal{K}} u_t = \int_{\mathcal{K}} u_s$. A global assembly is performed by volume-weighted averaging (Alauzet, Mehrenberger, 2009), and the target field can easily been deduced:

$$d_{t_i} = \frac{\sum\limits_{\mathcal{K}_j \in \{\mathcal{K}(w_{t_i})\}} |\mathcal{K}_j| d_{loc_t^i}}{\sum\limits_{\mathcal{K}_j \in \{\mathcal{K}(w_{t_i})\}} |\mathcal{K}_j|}, \quad (10)$$

where $\{\mathcal{K}(w_{t_i})\}$ represents the set of elements supporting the i$^{\text{th}}$ basis function, and $|\mathcal{K}_j|$ is the volume of the element. $d_{loc_t^i}$ is a local DoF computed using the equation (9). This method presents the advantage to reduce the local errors and behaves as global projection (Clement, 1975). Moreover no linear system is solved, thus simplifying the implementation and reducing the computational cost.

1.4. Importance of the numerical integration

Both the conservative and the orthogonal methods require the evaluation of the integral of u_s (equations (8b) and (9)) throughout a target element. An adaptive integration scheme was used as it presents the best trade-off between speed and accuracy. Therefore we have also implemented and tested three schemes: the "intersections", the "fixed high precision quadrature", and the "adaptive quadrature".

The computation of the intersections consists in the determination of all volumes created by the intersection of the two meshes. Thus the polynomial expression of $w_{t_i} \cdot w_{s_j}$ is well-defined and a classical quadrature rule can be used. However, distorted simplexes can be created during the intersection process leading to an inaccurate computation of equation (8b).

The second strategy uses a quadrature of high order in each target element. Depending on the variation of u_s through the considered element, the chosen quadrature can be not precise enough, or on the contrary too accurate (leading to computational overcosts).

Finally, the third strategy consists in the virtual split of the target element if the quadrature rule has not reached a predefined accuracy criterion. This process leads to an automatic adaption of the quadrature to the variation of u_s.

Computation errors depend on the source function and the meshes. Table 1 presents accuracies and computation times for given meshes and source function. Similar behavior is observed in all cases. However we do note the more the second derivative increases, the more the adaptive scheme is long to compute and the less the fixed quadrature is accurate.

Table 1. Computational times and accuracies for the different integration schemes

	Intersections	High precision quad.	Adaptive quad.
Global error (%)	0.402	0.378	0.369
Computation time (s)	38	0.4	0.8

2. Numerical test of the data transfer methods

The interpolation, conservative, and orthogonal data transfer methods are compared in terms of global conservation, as well as global and local errors. We have, in a first time, tested these methods using the discretized version of the analytical source function $u = (1 + r)^4$ which presents strong variations compared to the target mesh size. r is the radius of the spherical coordinates system. The figure 1 presents the two meshes used for the analytical computations. Meshes are based on cubes ranging from -1 to $+1$ in the three directions of the space. The source and target meshes are respectively composed of 200.000 and 22.000 tetrahedra.

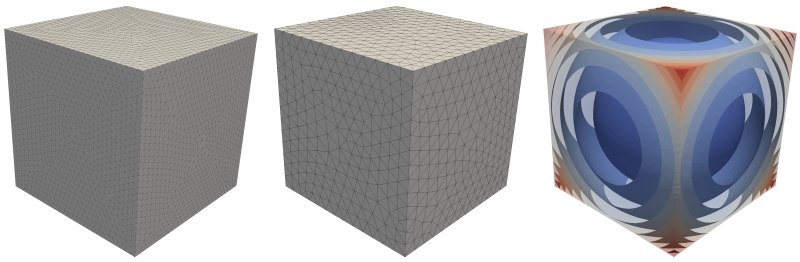

Figure 1. Representation of the two meshes and the isovalues of the field

Errors and computation times are presented in table 2 (for node elements), and are in accordance with the behavior of the different methods. The interpolation process is

not conservative as the global error is far greater than using the conservative and orthogonal methods, however this method is fast to compute and simple to implement. The two other methods produces similar results for local and global errors. The conservative method remains attractive because of its relative simplicity compared with the accuracy: no sparse matrix and linear system have to be handled.

Table 2. Local / global errors and computation times for the transfer of nodal functions

	Interpolation	Conservative	Orthogonal
ϵ_{global} (%)	1.347	0.378	0.369
ϵ_{local} (%)	1.508	0.762	0.713
t (s)	0.02	0.4	0.8

Thus the interpolation process can be used if the conservative aspect has little influence, or if no overshoots or undershoots are required. Otherwise, conservative and orthogonal methods are preferred.

3. Application to a magneto-thermal case

A conductive wire, under imposed voltage, is heated by Joule losses and the conductivity exponentially varies with the temperature (see figure 2). The purpose of this test case is to compute the steady state temperature distribution of this highly coupled problem, using the chaining defined in figure 3. The parameters of the model are listed in table 3.

Table 3. Parameters of the magneto-thermal problem

Parameters		
$R = 1\text{m}$	$H = 1\text{m}$	$V = 84.8528\text{V}$
$\rho\, C_p = 50\text{kJK}^{-1}\text{m}^{-3}$	$h = 50\text{Wm}^2$	$\lambda = 100\text{Wm}^{-1}\text{K}^{-1}$
$\sigma_0 = 0.4437\Omega^{-1}\text{m}^{-1}$	$T_a = 20°\text{C}$	$\theta = 50\text{K}$

V is an imposed voltage, $\rho\, C_p$ is the heat capacity, and λ is the thermal conductivity. The local conductivity and the flux of heat losses are given by:

$$\sigma = \sigma_0\, e^{(T-T_a)/\theta} \tag{11a}$$

$$\Phi_l = h\,(T - T_a) \tag{11b}$$

The stationary distribution of temperature can be determined analytically and gives values of $65.89°\text{C}$ at the center of the cylinder and $56.36°\text{C}$ on the lateral surfaces. The magnetic problem and the thermal problem were solved using two different meshes (see figure 4). Considering the geometry of the test case, the magnetic problem can easily been solved without the air domain (i.e the normal component of the magnetic field is null on the lateral surfaces of the cylinder, thus the appropriate boundary conditions can be applied here). However, an air domain has been added in order to

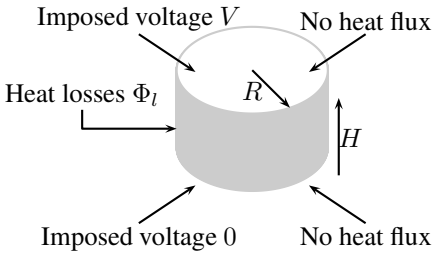

Figure 2. Sketch of geometry of the test case

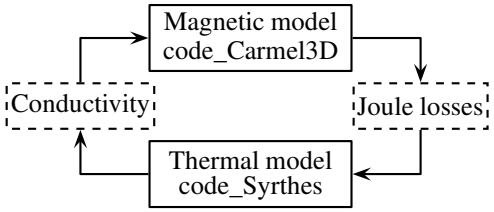

Figure 3. Flowchart used for the computation

complicate the coupling scheme as geometries are then topologically different. Local Joule losses are computed using the electric field ($\sigma|J|^2$) deduced from the electric scalar potential.

The three projection methods were tested to transfer the heat losses from the magnetic mesh to the thermal one. Magnetic Joule losses, constant by element, have been transferred to nodal values throughout the thermal domain. In all cases, an $\mathcal{L}^2$ projection is used to compute the actual distribution of the conductivity (knowing the temperature throughout the thermal domain) within the magnetic mesh. Both the conservative and orthogonal methods gives the same results as the preservation of the total heat power is more important than the modifications induced in the distribution of losses. The figure 5 presents the distribution of the temperatures for the interpolation process and the conservative / orthogonal projections. Numerical results for the center and lateral temperatures are given in table 4, results are compared with the analytical values.

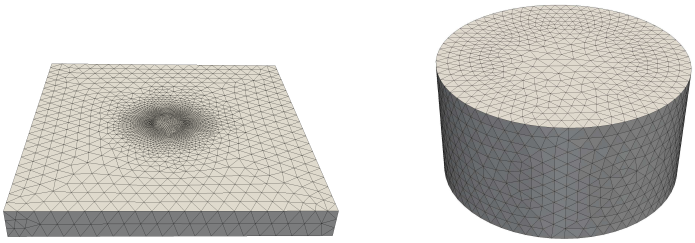

Figure 4. Magnetic mesh with air (left), and thermal mesh (right)

As visible in table 4, results obtained with the interpolation method are far from the analytical solution while the conservative / orthogonal methods are much more accurate. Because of the exponential variation of the conductivity with the temperature, simple interpolation methods could not be used here. The conservative nature of

Table 4. Errors on temperatures

	Reference		Interpolation		Cons. / Orth.	
	Center	Lateral	Center	Lateral	Center	Lateral
Temperature (°C)	65.89	56.36	53.63	46.11	65.56	56.06
Error (%)	–	–	18.6%	18.2%	0.5%	0.5%

the conservative and orthogonal methods enable an accurate computation despite the minor changes introduced in the distribution of the Joule losses.

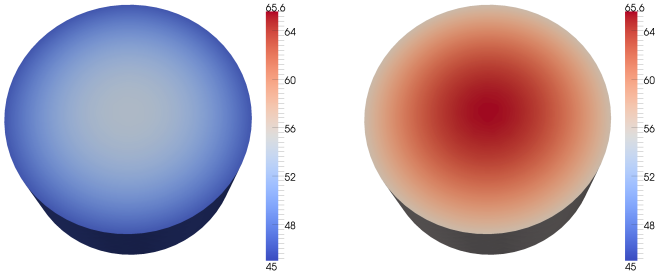

Figure 5. Temperature through the cylinder for the interpolation method (left) and the conservative / orthogonal method (right).

Remark:

These methods can also be applied to non-homogeneous materials. The prescribed integration rules do not change, however jumps and strong have to be handled with care (further details are provided in (Journeaux *et al.*, 2014)).

4. Conclusion

We have presented three type of mesh-to-mesh data transfer methods which have –considering their assets / weaknesses in terms of accuracy and computation cost– different scope of uses. The numerical tests of these methods have shown that the interpolation method, despite its frequent use, is strongly diffusive and can lead to inaccurate computations of coupled problems. The conservative and orthogonal methods have similar behavior. Moreover the small precision improvement provided by the orthogonal projection lead to more complex algorithms. The ability of the multi-meshes weak coupling schemes to model coupled problem has been shown on an analytical test case.
The mesh-to-mesh data transfers have successfully been applied to magneto-thermal, magneto-mechanical, and magneto-thermo-mechanical (Nemitz *et al.*, 2011; Journeaux *et al.*, 2013) cases. This study is part of the development of a generic coupling tool, `code_Interpol`, a software which implements four types of data transfer methods,

parallel computations of intersections as well as an adaptive integration technique, and is used by the EDF company to solve multi-physics problems.

Acknowledgements

This study would not have been possible without the helpful work of J.Y. Roger, research engineer at EDF R&D.

References

Alauzet F., Mehrenberger M. (2009). *P1-conservative solution interpolation on unstructured triangular meshes*. Rapport de recherche No. RR-6804. INRIA. Retrieved from http://hal.inria.fr/inria-00354509

Bernardi C., Maday Y., Patera A. (1993). Domain decomposition by the mortar element method. In H. G. Kaper, M. Garbey, G. W. Pieper (Eds.), *Asymptotic and numerical methods for partial differential equations with critical parameters*, Vol. 384, p. 269-286. Springer Netherlands. Retrieved from http://dx.doi.org/10.1007/978-94-011-1810-1_17

Clement P. (1975). Approximation by finite element functions using local regularization. *NUMDAM: Revue française d'automatique, informatique, recherche opérationnelle. Analyse numérique*, Vol. 9, No. 2, pp. 77-84.

Hameyer K., Driesen J., De Gersem H., Belmans R. (1999). The classification of coupled field problems. *Magnetics, IEEE Transactions on*, Vol. 35, No. 3, pp. 1618-1621.

Jiao X., Heath M. T. (2004). Common-refinement-based data transfer between nonmatching meshes in multiphysics simulations. *International Journal for Numerical Methods in Engineering*, Vol. 61, pp. 2402–2427.

Journeaux A. A., Bouillault F., Roger J.-Y. (2013, 2). Multi-physics problems computation using numerically adapted meshes: application to magneto-thermo-mechanical systems. *The European Physical Journal - Applied Physics*, Vol. 61. Retrieved from http://www.epjap.org/action/article_S1286004213400988

Journeaux A. A., Nemitz N., Moreau O. (2014). Locally conservative projection methods: benchmarking and practical implementation [Article]. *Compel-The International Journal For Computation And Mathematics In Electrical And Electronic Engineering*, Vol. 33, No. 1-2, pp. 663-687.

Nemitz N., Moreau O., Ould-Rouis Y. (2011, july). Magneto-thermal coupling: A conservative-based method for scalar field projection. In *18th Conference on the Computation of Electromagnetic Fields (Compumag 11), Sydney, Australia, Jul 12-15, 2011,*, Vol. 18.

Ren Z., Razek A. (1994, apr). Modelling of dynamical behaviours of electro-magneto-mechanical coupled systems. In *Computation in electromagnetics, 1994. second international conference on*, p. 20 -23.

Tsukerman I. (1992). Overlapping finite elements for problems with movement. *Magnetics, IEEE Transactions on*, Vol. 28, No. 5, pp. 2247-2249.

Received at 23 March 2014
Accepted at 15 May 2014